International Journal of GEOMATE, Nov., 2020, Vol.19, Issue 75, pp.92-99
ISSN: 2186-2982 (P), 2186-2990 (O), Japan, DOI: https://doi.org/10.21660/2020.75.55587
Geotechnique, Construction Materials and Environment

MUD ERUPTION DYNAMIC IN CIUYAH, JAVA, INDONESIA

*Vijaya Isnaniawardhani[1], Nanda Natasia[2], Titin Kartina Effendi[3], Boy Yoseph Cahya Sunan Sakti Syah Alam[4], Ismawan[5] and Nana Sulaksana[6]

[1,2,5] Department of Geosciences, Universitas Padjadjaran, Indonesia
[3,4,6] Department of Applied Geology, Universitas Padjadjaran, Indonesia

*Corresponding Author, Received: 15 April 2020, Revised: 06 May 2020, Accepted: 29 July 2020

ABSTRACT: This study concerns the activities, forms, and spread of mud eruption in Ciuyah as a part of Java-Madura axial depression zone. Landsat interpretation and detailed field observation were conducted to find out the eruption activity, the conduit system, and the host rock. Both physical and chemical properties of erupted material were tested to track down the mud origin, movement dynamic, and changes during transportation. Active bubbling which bring fluid, claystone- to sandstone-size solid particles, gas, and heat as well as crusting material inside conduits are detected in Ciuyah. The high similarity of rock composition and fossil contained indicated that the mud comes far below the surface passes the rock layers of the Late Tertiary sedimentary rock (Pemali and Halang Formations), and then ejected to the surface through conduits. The temperature of extruded mud reaches 6.9° to 13.6° compared to air temperature (hyperthermal). Conduits where the mud comes out mostly show NW-SE direction as a minor pattern of existing morphological lineament directions. Changes seen in pH, TCD and EC, besides hydro-chemical composition (level of Na^+, Cl^-, SiO_2, Mn^{2+}, K^+, Li^+, Fe^{3+}, Mg^{2+}, HCO_3^-, Ca^{2+} and SO_4^-) caused by water formation as well as minerals enrichment dissolved due to heat and long-time contact to the side rock during eruption.

Keywords: Mud eruption, Ciuyah, Erupted material, Lineament

1. INTRODUCTION

Mud eruption is known as the packets of fluid-containing suspension materials piercing upward from subsurface to the Earth's surface due to buoyancy and differential pressure. It has attracted the attention of geologists for over two centuries. These phenomena are found almost everywhere on Earth. They are associated with rapid deposition, lateral tectonic compression with overpressure and geologically recent magmatic activity [1].

Mud eruptions are found along the depressions of Java to Madura in Bogor-North Serayu-Kendeng-Madura Strait Zone in Fig.1 such as Ciuyah (Kuningan, Eastern West Java), North Serayu (northern Central Java), Bledug Kuwu, Bledug Kesongo, Bledug Kropak (to the south of Purwodadi, Central Java), Sangiran Dome (Central Java), LUSI (abbreviation of "Lumpur Sidoarjo" or Sidoarjo Mud, East Java), Karang Anyar, Pulungan (Sidoarjo), Gunung Anyar (Surabaya), Socah (Bangkalan, Madura), and Madura Strait. They occur in an "elisional" basin mainly characterized by quick and stable tectonic submergence resulted in the rapid deposition of ultrathick (up to 15 km) young sedimentary series, fluid overpressure presences, under-compacted sediments, and petroleum generation, which then recently tectonically compressed [2-4].

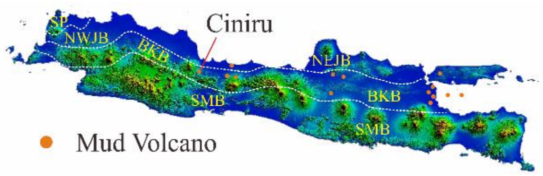

Fig.1 Ciuyah and other mud eruptions, represented by orange dots, are situated along the Bogor-North Serayu-Kendeng-Madura Strait depositional center zone (SP: Sunda Platform, NWJB: North West Java Basin, NEJB: North East Java Basin, BKB: Bogor-Kendeng Basin, and SMB: Southern Mountain Basin)

In Ciuyah, approximately 5 km south of Kuningan Regency in the district of Ciniru, the mud eruption occurred continuously in at least 22.5 ha square. Although the mud outflow is insignificant, it spread widely since it has been going on for a long time. The origin of Ciuyah mud eruption, like the LUSI (the world's largest mud eruption that has been in eruption since May 2006), bring out many questions.

Ciuyah mud eruption occurs within the axial depression of Java to Madura (the Bogor-North Serayu-Kendeng Trough). This site has been trending parallel to the tectonic compression due to the subduction of Indian Oceanic crust to the south of Java and coeval volcanic arc [5]. In this zone, Miocene to Pleistocene marine sediments were rapidly deposited and under compacted. It has been compressed and uplifted since the Plio-Pleistocene time. The morphological features of this area are mainly controlled by tectonic activities. Quaternary volcanic rock and alluvium have covered some places [2,6,7].

In Recent studies, the appearance of mud eruptions is often associated with earthquake [8,9].

This study focuses on activities, forms, and spread of mud eruption in Ciuyah. The conduit system plays an important role in the mud eruption process. [10]. A discussion on physical and chemical properties of mud follows. Integrated analysis on the nature of the eruption and the particles in the mobilized mud will address the nature of mud eruption dynamics.

Eruption activity in Ciuyah has occurred for long time. It is predicted to continue for the next years. Triggered by seismicity, a large amount of erupted mud becomes serious environmental issues in the future if not managed immediately [1, 11-15].

2. METHODS

There are various approaches to mud eruption identification that can be divided into geological, tectonic, and hydrogeological methods, most of which are interrelated [16]. Many studies applied different methods which are interconnected to find out the origin, depth of source, age, product, spread, and dynamics of the eruption. A combination of physical characteristics of mud, mineralogy and grain-size clasts, fossil content, water content, and geometry of the eruption were analyzed to reconstruct mud evolution [17]. Similar techniques have been used in other studies to constrain either the origin of mud or mud flow periodicity with a very good results [18-20].

Some approaches were applied in this study that focused on exposing the phenomenon of mud eruption spread in Ciuyah, administratively under the jurisdiction of the Ciniru District, 25 km southeast from the government seat of Kuningan Regency, the Province of West Java.

The study was done in several stages, starting from literature review, followed by field observation, sampling, laboratory analysis, and studio work. Landsat imagery (ASTER Global Digital Elevation Model from the USGS Earth Explorer) was used in the analysis to enhance the understanding of morphological patterns.

Detailed geological field observation was conducted to find out the host rock, conduit system, and eruption activity. Moreover, a compilation of Landsat interpretation and field data can be used as a guide to find out the stress orientation and tectonic pattern which control the eruption process [21].

Exposed host rocks were collected for petrological and paleontological laboratory analysis. The size of the solid material contained is measured by a sieve test for coarse grains and hydrometer test for fine grains. The host rock and mud particles that flowed to the surface were observed using a microscope to determine physical and biological characteristics.

The quantitative approach is used to determine the similarity between the mud and its source. Previous literatures proposed estimation of similarity based on diversity index (H), evenness index (e), and similarities index (SI) [22,23].

To determine the origin of mud, the similarity index of material contained in mud with host rock is calculated using the equation below:

$$\mathrm{H} = \sum \mathrm{pi} \log p; \text{with } \mathrm{pi} = \frac{ni}{N} \tag{1}$$

H = Shannon-Weaver's Diversity Index
ni= the significant index- or the abundance- of each type
N = the significant index- or the abundance- of all types

$$\mathrm{e} = \frac{H}{LogS} \tag{2}$$

e = evenness index
S = number of types

$$IS = \frac{C}{A+B-C}\, x\, 100\% \tag{3}$$

IS = similarity index
A = the number of types only found in mud
B = the number of types only found in rock
C = the number of types found in mud and rock

The liquid erupted material was sampled inside center of the conduit or crest. Temperature as well as physical properties of mud flow (pH, total dissolved solid/TDS, and electrical conductivity/ EC) were directly measured on site. Meanwhile the chemical properties of fluid (cation-Ca^{2+}, Mg^{2+}, Fe^{3+}, Mn^{2+}, K^{+}, Na^{+}, Li^{+}, anion-HCO_3^-, Cl^-, SO_4^-, and neutral-SiO_2) was laboratory tested. The analysis will reveal the genesis or source of fluid and enrichment during transportation [24]. In addition to mud, some samples from water springs and wells were also analyzed as comparison.

The integrated field observation and laboratory data serve as a guide to find out the dynamics of mud eruption. This phenomenon is approached based on the source, migration, product, and spread of mud.

3. RESULT

The oldest rocks exposed in Ciuyah is Middle Miocene claystone facies a part of the Pemali Formation composed of thick beds of deep marine calcareous claystone with silt, sandstone, and limestone intercalations. This fine grain facies are overlain by Middle to Pliocene sandstone facies of the Halang Formation which consists of sandstone, conglomerate, silt, and claystone. Tectonic activities had uplifted this succession so that it could be observed in the surface. It is covered by Quaternary volcanic rocks and alluvium. These thick host rocks were rapidly deposited and compressed to become fold and thrust belt during the Mio-Pliocene and Plio-Pleistocene eras. Since then, recent volcanic activity triggered the development of mud eruption occurs in Ciuyah area [6].

3.1 Eruption Activity Stages

Waluyo (2007) proposed four stages of mud eruption, initiated by the embryonic stage (mud deformation at weak zones below the surface), diapirism (mud moving upwards approaching the surface), mud eruption (mud emergence on the surface), and terminated by the post-eruption (partial subsidence beneath mud complex due to decrease in subsurface pressure) [2]. Active bubbling mud in Ciuyah demonstrates stage-3 mud eruption activity (syn-eruption) (Fig.2). At the same places, fresh materials without mud bubbling or flow are recorded to be present inside the rest of the outlet points. The vibrating mud crust covered by vegetation is sometimes extruded or removed due to the reactivation of mud movement or elution. Fresh and crusting materials as well as hard residual materials reflected stage-4 (post-eruption) or dormant.

Fig.2 Bubbling mud flow out to the surface indicates stage-3 on eruption activity

3.2 Morphology

3.2.1 Conduit and crest

The conduit is defined as a central feature through which mud eruption facilitated upward migration mass from the depth [10]. It was spread out at an elevation of 256 to 325 m in Ciuyah. Three conduit shapes (oval, slit and irregular) are observed on the surface, varying from several centimeters to half a meter in diameter. They show positive, negative or flat features. The small diameter holes (< 10 cm) in groups have formed elongated cluster patterns. At some places, the central conduit appeared as the most elevated point or cropped out in the surface known as the crest.

3.2.2 Surface morphology

Based on surface morphological types of mud eruption proposed by Akhmanov and Mazzini (2007) [2], there are three types of mud eruption surface morphology in Ciuyah, namely classic mud cone, crater muddy lake and swamp-like area, as explained bellow:

a. classic mud cone
   The positive featured cone with main crater and stratification of mud layers which have a conical or volcano-like shape is built during eruption. The stratification usually formed few cm to 20 cm high dense flat or sloping beds stacking periodically accumulating around the conduit.

b. crater muddy lake
   The reduction in subsurface pressure resulted in partial collapse inside the conduit system and formed depression features or crater lakes.
c. swamp-like area

   Active eruptions ejected fluid-rich mud with gas bubbles swamp large areas. Some of outlet have been enclosed by crust or vegetation. Generally, the long axis of conduits indicates the direction of E-W (Fig.3).

Fig.3 Mud flows from several outlets continuously formed a wide swamp-like area in E-W direction

3.3 Erupted Materials

In the Ciuyah mud complex, active holes release fluid, claystone to sandstone-size solid particles (rock fragments and microfossils), gas, and heat [25]. The characteristics of those erupted materials will be compared to surficial as well as side and base-elements of Pemali and Halang Formations as described below.

3.3.1 Heat

The water temperature measured on nine natural water springs and man-made water wells shows ranges from 26.2° to 29.4°C. Those data are lower than the air temperature degrees ranging from 27.9 ° to 29.8° C. Meanwhile extruded mud temperature measured on six observation points ranging from 34.8° to 43.4° C are higher than the air temperature (hyperthermal).

3.3.2 Rock fragments

Grain size analysis on mud identified that the solid particles are mostly fine grain (more than 85%) in clay-sized grain about 50-65% mixed with silt-sized grain about 20-35%. The coarse grain portion is less than 15% sand-size materials. The particles consist of sedimentary and igneous rocks.

Microscopic analysis on mud and rock indicated similarities on type, texture, and mineral composition between rock fragments erupted to the surface and the base and side-rock (Table 1, Fig.4).

Table 1 Lithologic composition of host rock of Pemali and Halang Formation and rock fragments in mud

Lithology	Host Rocks	Rock Fragments in Mud
Claystone (clastic sedimentary rock)	Grey, brown. Fragment (5-25%): fossils, quartz, glauconite, mica, feldspar, opaque minerals. Matrix and cement (75-95%): clay.	Brown, reddish brown. Fragment (4-20%): fossils, quartz, glauconite, mica, felspar, opaque minerals. Matrix and cement (80-96%): clay.
Sandstone (clastic sedimentary rock)	Grey to brown, feldsparthic graywacke. Fragment (25-85%): rock fragments, quartz, K-feldspar, mica, plagioclase, amphibole, pyroxene, opaque minerals. Matrix and cement (15-75%): clay, feldspar, quartz, secondary minerals.	Grey, feldsparthic graywacke. Fragment (24-44%): rock fragments, quartz, mica, K-feldspar, plagioclase, amphibole, pyroxene, opaque minerals. Matrix and cement (56-76%): clay, feldspar, secondary minerals.
Limestone	Bioclastic wackestone and packstone, whitist, yellowish, light brown, compact, fine to very coarse grain size. Grain (30 – 55%): fossils, carbonate minerals, glauconite, quartz and sedimentary rocks. Matrix (45-70%): mud, carbonate micrite, secondary minerals.	Bioclastic wackestone, light to dark to brown, Grain (35%): fossils, carbonate minerals, glauconite, quartz and sedimentary rocks. Matrix (65%): Mud, carbonate micrite, secondary minerals.
Andesite (igneous rock)	Blackish-brown and greenish, porphyritic-porphyro-aphanitic. Phenocrysts: plagioclase, biotite, quartz, hornblende, pyroxene, and opaque minerals (63 – 78%). Groundmass (22-37%): plagioclase, quartz	Blackish-brown and dark grey, porphyro-aphanitic. Phenocrysts (70%): quartz, muscovite, K-feldspar, plagioclase, biotite, hornblende, pyroxene, and opaque minerals Groundmass (30%): plagioclase, quartz

Table 1 continues to the next page

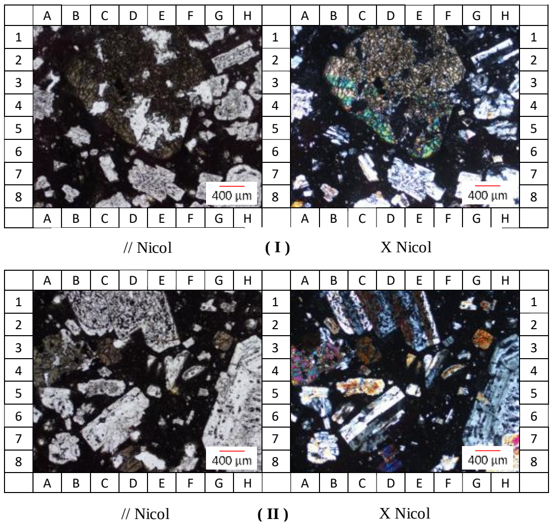

Fig.4 Thin sections of feldsparthic sandstone of rock fragments in mud (I) as well as host rock (II) present similar textures and mineral content

3.3.3 Microfossils content

Late Tertiary marine sedimentary rock of Pemali and Halang Formations in Ciniru contains foraminifera. There is a total of 84 foraminiferal species can be identified in the rock samples, half of which are planktic while the others are benthic (Table 2).

Table 2 Quantitative data on foraminifera assemblages in mud and host rock samples

Descriptions	Host Rock	Mud
Number of determined species	84	75
Number of determined planktic species	42	38
Number of determined benthic species	42	37
Average species abundancy	165.71	71.43
Average species number	37	35.29
Average diversity index	1.35	1.45
Average evenness index	0.90	0.96

Thirty-eight planktic (90.48%) and thirty-seven benthic species (88.10%) are found in mud ejected from the subsurface [25]. Based on the quantitative analysis of foraminifera assemblages, the similarity index of both groups is 89.29%.

3.3.4 Fluid

Physical and hydro-chemical laboratory analyses on spring fresh water and extruded mud demonstrate that there is variety in physical and chemical properties. The physical properties as pH, TDS and EC values measured in ejected mud are higher than fresh water (Table 3).

Table 3 The comparison of physical properties between spring water and extruded mud

Descriptions		Fresh Water	Extruded Mud
pH	range:	6.3 to 7.1	6.7 – 7.2
	average:	6.72	6.88
TDS (mg/l)	range:	140 to 290	119 – 177
	average:	213.33	155.67
EC (µS/cm)	range:	300 to 590	223 – 403
	average:	447.78	326.33

In fresh water, the total of solids dissolved in water (TDS) and the electrical conductivity of water (EC) are in a close relationship. The differences amount of metals, minerals and salts that more or less conductive than others will influence the value of EC. As seen in Fig.5, the trend of fresh water and erupted mud data is different.

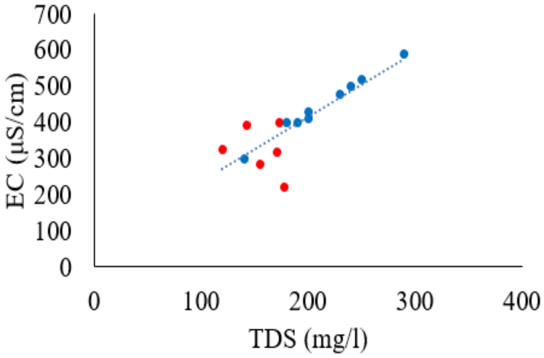

Fig.5 TDS vs EC points of fresh water, represented by blue dots, plotted as a single straight line means that TDS rise is proportional to EC. In contrast, nonlinear relationship is shown by ejected mud represented by red dots

Hydro-chemical laboratory records (Ca^{2+}, Mg^{2+}, Fe^{3+}, Mn^{2+}, K^{+}, Na^{+}, Li^{+}, HCO_3^{-}, Cl^{-}, SO_4^{-}, and SiO_2) on fresh water and extruded mud samples show significant difference values (Table 6). In general, cation and anion in ejected mud are higher than fresh water.

Table 4 Hydro-chemical composition in spring water and extruded mud samples

Description		Fresh Water	Extruded Mud
Ca^{2+} (meg/l)	range:	1.94 to 5.86	12.96 to 17.60
	average	3.26	15.82
Mg^{2+} (meg/l)	range:	0.70 to 1.23	26.02 to 32.12
	average	0.99	28.82
Fe^{3+} (mg/l)	range:	0.12 to 0.61	6.98 to 12.30
	average	0.34	9.63
Mn^{2+} (mg/l)	range:	0.05 to 0.07	2.14 to 5.61
	average	0.06	3.28
K^{+} (meg/l)	range:	0.02 to 0.36	5.47 to 5.87
	average	0.13	5.70
Na^{+} (meg/l)	range:	0.78 to 1.97	393.91 to 399.32
	average	1.10	397.27
Li^{+} (mg/l)	range:	0.16 to 0.74	15.31 to 15.68
	average	0.43	15.50
HCO_3^{-} (meg/l)	range:	3.22 to 6.55	49.92 to 52.68
	average	4.59	51.34
Cl^{-} (meg/l)	range:	0.36 to 1.10	344.64 to 396.30
	average	0.57	368.91
SO_4^{-} (meg/l)	range:	0.32 to 1.12	0.99 to 1.27
	average	0.77	1.15
SiO_2 (mg/l)	range:	0.54 to 0.74	49.8 to 53.8
	average	0.65	51.40

The ejected mud is enriched in Na^{+}, and Cl^{-} compared to fresh water. The concentration of Na^{+} in mud is about 360 times higher than fresh water meanwhile the concentration of Cl^{+} about 650 times. The hydro-chemical data of fresh water plotted in Piper's diagram (trilinear diagram) grouped into Ca-Mg-HCO_3 facies in the volcanic aquifer system. The significant elevate of Na^{+} and Cl^{-} contents causes change of mud facies to Na-K-Cl (Fig. 6).

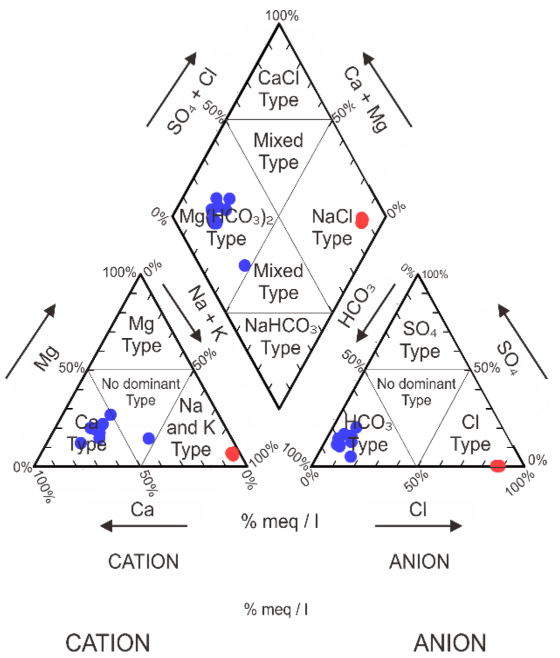

Fig.6 Hydro-chemical composition on samples plotted in Piper's diagram show the differences in the facies fresh water (represented by blue dots) and ejected mud (represented by red dots).

3.3.5 Gas

Pressurized gas released though the conduit system produces bubbling mud. The gas expelled is non-flammable such as CO_2 with traces of H_2S.

3.4. Lineament

The lineaments observed in Landsat imagery as manifestation of 247 ridges and 129 valleys orientation (Fig 8). There are grouped in 8 trends (Table 5), namely N-S, NNE-SSW, NE-SW, ENE-WSW, E-W, ESE-WNW, SE-NW and SSE-NNW. The total 450.5 km length of ridge lineaments is dominated by East-West trend along 119.5 km. The total 358.5 km length of the valley is also dominated by the same trend along 102 km.

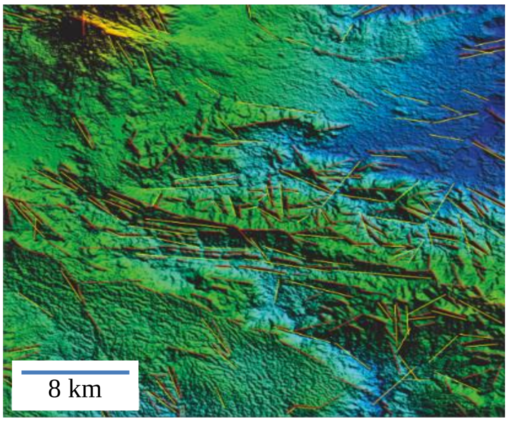

Fig.8 Ridge and valley lineaments used for Landsat imagery interpretation

Table 5 Lineament trends in Ciniru area

Lineaments	Length (km) < 1	1 – 2	2 – 3	3 – 4	4 – 5	> 5
Ridge Lineaments						
N-S	2	4	4			
NNE–SSW		5				
NE–SW	1	4	2	2		
ENE–WSW	1	15	5	3		
E–W	8	32	13	5	3	1
ESE–WNW	10	29	12	5	1	1
SE–NW	7	31	9	1	1	
SSE–NNW	3	17	8	2		
Valley Lineaments						
N-S		4	2	2		
NNE–SSW		2	2	1		
NE–SW	1	3	1	1	2	
ENE–WSW		3	2	3		
E–W		8	10	5	2	7
ESE–WNW		3	11	8	1	2
SE–NW		4	9	7	1	
SSE–NNW		7	9	6		

Based on Landsat imagery interpretation the lineament patterns that reflected orientations of rock layer are dominated in ENE–WSW (51 from 133 measurements).

4. DISCUSSION

The presently still occurring eruption activity bring to the surface claystone-size to sandstone-size solid particles (rock fragments and microfossils), gas, and heat. The temperature of the extruded mud is higher compared to the air temperature (hyperthermal).

The similarity of rock composition and fossil contained in mud and Late Tertiary sedimentary rock (Halang and Pemali Formations) indicates that the mud comes from far below the surface passing the rock layers which has been formed before then ejected to the surface through conduits [25].

Landsat imagery interpretation finds extending ridge and valley lineaments in the Ciniru area with ENE-WSW major direction. Detailed surface mapping focusing on the structural geology records that the fold axials appears to be in line with imprint directions of the morphological lineament [6]. Data in the field shows that the long axis orientation and the distribution of conduits is mostly in NW-SE-ward, with minor WSW-ENE and NE-SW-wards. The difference of the conduit pattern with both dominant directions is assumed that they are controlled by a minor pattern.

Extruded mud has a different pH, TDS and EC value compared to the fresh water. Further analysis shows nonlinear relationship between TDS and EC. Dissolution of the elements in the rock traversed has caused high levels of Ca^{2+}, Mg^{2+}, Fe^{3+}, Mn^{2+}, K^{+}, Na^{+}, Li^{+}, HCO_3^{-}, Cl^{-}, SO_4^{-}, and SiO_2 contained in extruded mud. High amounts of Na^{+} dan Cl^{-} are supplied by formation water contained inside host and side rock (marine sediment Pemali dan Halang Formations). Increased Ca^{2+} levels are caused by dissolved calcite minerals found in claystone and carbonate sandstones from the traversed rocks. In a line, the increase in SiO_2, Mn^{2+}, K^{+}, Li^{+}, Fe^{3+}, HCO_3^{-} and SO_4^{-} is caused by dissolved rock elements while Mg^{2+} comes from the exchange of calcium ions contained in the sedimentary rocks. The heat flowing along with the mud material has accelerated this process during mobilization [24].

5. CONCLUSION

Active bubbling and crusting material inside conduits are detected in Ciuyah. Fluid, claystone- to sandstone-size solid particles, gas, and heat are released from active conduits. The temperature of extruded mud is 6.9° up to 13.6° degrees higher than the air temperature. The size and mineral composition of rock fragments as well as foraminifera content in extruded mud show high similarities (more than 85%) with the Late Tertiary sediment host and side rocks (Pemali and Halang Formations).

TDS vs EC from erupted mud shows nonlinear relationship. The level of mud is higher than that of fresh water. This indicates that enrichment has occurred in the mud all the way to the surface due to the dissolution of rock-forming elements in its path.

Mud comes to the surface through conduits with E-W orientation as minor direction of existing ridge and valley lineament patterns.

The water formation, heat, and longtime contact to side rock have caused minerals enrichment to dissolve during eruption.

6. ACKNOWLEDGEMENTS

We would like to express our gratitude to the Rector of Universitas Padjadjaran for the research grant. We are also grateful for the great support from colleagues in deep discussion as well as students in conducting field work and laboratory analysis.

7. REFERENCES

[1] Milkov A.V., Global Distribution of Mud Volcanoes and Their Significance as an Indicator of Active Petroleum Systems, A Source of Methane in The Atmosphere and Ocean, and A Geohazard, Conference paper, in “Mud Volcanism, Geodynamics, and Seismicity”, 2003, pp.29-34.

[2] Satyana A.H., and Asnidar Mud Diapirs and Mud Volcanoes in Depression of Java to Madura: Origin, Natures and Implication to Petroleoum System, Conference proceedings, in Proc. 32nd Annual Convention and Exhibition Indonesian Petroleoum Association, 2008, pp.139-158.

[3] Istadi B.P., Wibowo H.T., Sunardi E., Hadi S., and Sawolo N., Mud Volcano and its Evolution, in Earth Sciences, in Tech, 2012, pp.375-434.

[4] Wibowo H.T., Prastisho B., Prasetyadi C., and Yudiantoro D.F., The Evolution of Sidoarjo Hot Mudflow (Lusi), Indonesia, IOP Conf. Series: Earth and Environmental Science 212, 2018, pp.1-11, https://doi:10.1088/1755-1315/212/1/012050.

[5] Hall R., Clements B., Smyth H.R., and Cottam M.A., A New Interpretation of Java’s Structure, in Proc. 31st Annual Convention and Exhibition Indonesian Petroleum Association, 2007, pp.35-57.

[6] Isnaniawardhani V., Helmi F., and Muhammadsyah F., Stratigraphy and Structural Geology of Ciuyah Mud Volcanoes in Ciniru Area, West Java, International Journal of Science and Research, Vol. 4, Issue. 4, 2015, pp.3223-3226.

[7] Muhammadsyah F., Sunardi E., and Isnaniawardhani V., Karakteristik Geologi Daerah Gunungan Lumpur Ciuyah, Bulletin of Scientific Contribution, 10(2), 2012, pp.59-76.

[8] Menapace W., Kopf A., Zabel M., and Beer D., 2017, Mud Volcanoes as Phenomena that Host Marine Ecosystem, Life at Vents and Seeps, Berlin, Boston: de Gruyer, 2017, pp.53-84.

[9] Bonini M., Seismic Loading of Fault Controlled Fluid Seepage Systems by Great Subduction Earthquakes, Scientific Reports, Vol. 9, No.1, 2019, pp.1-12.

[10] Kopf A.J., Significance of Mud Volcanism, Review of Geophysics, Vol. 40, No. 2, 2002, pp. 1-52, doi.org/10.1029/2000RG000093.

[11] Maestrelli D., Bonini M., Delle D.D., Manga M., Piccardi L., and Sani P., Dynamic Triggering of Mud Volcano Eruption During the 2016-2017 Central Italy Seismic Sequence, Journal of Geophysical Research: Solid Earth, AGU Publication, Vol.122, 2017, pp.9149-9165, https://doi.org/10.1002/2017JB014777.

[12] Istadi B.P., Pramono G.H., Sumintadireja P., and Alam S., Modeling Study of Growth and Potential Geohazard for LUSI Mud Volcano, East Java, Indonesia, Marine and Petroleum Geology, Vol. 26, 2009, pp.1724-1739.

[13] Kure S., Winarta B., Takeda Y., Udo K., Umeda M., Mano A., and Tanaka H., Effect of Mud Flows from LUSI Mud Volcano on the Porong River Estuary, Indonesia, Journal of Coastal Research: Special Issues 70 – Proceedings of the 13th International Coastal Symposium, 2014, pp.568-573, https://doi.org/10.2112/S170-096.1.

[14] Handoko L., Yasufuku N., Ishikura R., and Rifa’i A., Comparison of Consolidation Curves for Remolded Mud Volcano of Sidoarjo, Indonesia, International Journal of GEOMATE, June, Vol. 10, Issue. 22, 2016, pp.1978-1982.

[15] Hidayati D., Ismail B.S., Shuhaimi-Othman M., and Sulaiman N., Chemical Composition of Mud Volcano LUSI and the Health Risk Involved Based on The Air Quality Index that Occurred as a Result of Disastrous Gas Exploration Drilling Activities in Sidoarjo, Indonesia, Sains Malaysiana, Vol. 47, No. 8, 2018, pp.1165-1674.

[16] Milkov A.V., Worldwide Distribution of Submarine Mud Volcanoes and Associated Gas Hydrates, Marine Geology, Vol. 167, Issues 1-2, 2000, pp.29-42, doi.org/10.1016/S0025-3227(00)00022-0.

[17] Menapace W., Tangunan D., Maas M., Williams T., and Kopf A., Rheology and Biostratigraphy of the Mariana Serpentine Muds Unravel Mud Volcano Evolution, Journal of Geophysical Research: Solid Earth / Vol. 124, Issue 11, 2019, pp.110-117, https://doi.org/10.1029/2019JBO18265.

[18] Collignon M., Schmid D.W., Galerne C., Lupi M., and Mazzini A., Modelling Fluid Flow in Clastic Eruptions: Application to the Lusi Mud Eruption, Marine and Petroleum Geology, Vol. 90, 2018, pp.173-190.
[19] Fryer P., Gharib J., Ross K., Savov and Mottl M.J., Variability in Serpentinite Mudflow Mechanisms and Sources: ODP Drilling Result on Mariana Forearc Seamounts, AGU Journals, Advance Earth and Space Science, Vol. 2, Issue 8, 2006, pp. 2-13.
[20] Fryer P., 2012, Serpentinite Mud Volcanism: Observation, Process, and Implications, Annual Review of Marine Science, Vol. 4, 2012, pp.345-373.
[21] Bonini M., Mud Volcanoes: Indicators of Stress Orientation and Tectonic Controls, Earth-Science Reviews, 115(3), 2012, pp.121-152.
[22] Ludwig J.A., and Reynolds J.F., Statistical Ecology: A Primer on Methods and Computing, John Wiley and Sons, 1988, pp.112-120.
[23] Barbour G.M., Burk J.H., Pitts W.D, Gilliam F.S., and Schwartz M.W, Terrestrial Plant Ecology, New York, The Benyamin/Cummings Publishing Company, Inc., 1980, 604 pp.211-239.
[24] Nicholson K., Geothermal Fluid Chemistry and Exploration Technique, Springer-Verlag, 1993, 263 pp.27-34.
[25] Isnaniawardhani V., Muhammadsyah F., and Sudradjat A., Foraminifera Assemblages as A Marker of Mud Eruption Source in Ciuyah, Ciniru – Kuningan, West Java, Riset Geologi dan Pertambangan,28, No. 2, 2018, pp.239-49.